



HAL
open science

A glutathione-dependent control of the indole butyric acid pathway supports Arabidopsis root system adaptation to phosphate deprivation

José A Trujillo-Hernandez, Laetitia Bariat, Tara A Enders, Lucia C Strader, Jean-Philippe Reichheld, Christophe Belin

► To cite this version:

José A Trujillo-Hernandez, Laetitia Bariat, Tara A Enders, Lucia C Strader, Jean-Philippe Reichheld, et al.. A glutathione-dependent control of the indole butyric acid pathway supports Arabidopsis root system adaptation to phosphate deprivation. *Journal of Experimental Botany*, 2020, 71 (16), pp.4843 - 4857. 10.1093/jxb/eraa195 . hal-03039133

HAL Id: hal-03039133

<https://univ-perp.hal.science/hal-03039133>

Submitted on 3 Feb 2021

HAL is a multi-disciplinary open access archive for the deposit and dissemination of scientific research documents, whether they are published or not. The documents may come from teaching and research institutions in France or abroad, or from public or private research centers.

L'archive ouverte pluridisciplinaire **HAL**, est destinée au dépôt et à la diffusion de documents scientifiques de niveau recherche, publiés ou non, émanant des établissements d'enseignement et de recherche français ou étrangers, des laboratoires publics ou privés.

A Glutathione-dependent control of IBA pathway supports Arabidopsis root system adaptation to phosphate deprivation.

José A. Trujillo-Hernandez^{1,2}, Laetitia Bariat^{2,1}, Tara A. Enders^{3,4}, Lucia C. Strader³, Jean-Philippe Reichheld^{2,1} and Christophe Belin^{1,2,*}

¹ Univ. Perpignan Via Domitia, Laboratoire Génome et Développement des Plantes, UMR 5096, F-66860, Perpignan, France.

² CNRS, Laboratoire Génome et Développement des Plantes, UMR 5096, F-66860, Perpignan, France.

³ NSF Science and Technology Center for Engineering Mechanobiology, Department of Biology, Washington University in St. Louis, St. Louis, MO 63130, USA

⁴ present address: Hofstra University, Department of Biology, Hempstead, NY11549, USA

*Corresponding author

E-mail: christophe.belin@univ-perp.fr

tel. +33 4 68 66 17 54

© The Author(s) 2020. Published by Oxford University Press on behalf of the Society for Experimental Biology.

This is an Open Access article distributed under the terms of the Creative Commons Attribution License (<http://creativecommons.org/licenses/by/4.0/>), which permits unrestricted reuse, distribution, and reproduction in any medium, provided the original work is properly cited.

Highlight

Arabidopsis root responses to IBA, but not IAA, depend on glutathione levels, and endogenous IBA and glutathione are both required for root system adaptation to phosphate starvation.

Accepted Manuscript

Abstract

Root system architecture results from a highly plastic developmental process to adapt to environmental conditions. In particular, the development of lateral roots (LR) and root hair (RH) growth are constantly optimized to the rhizosphere properties, including biotic and abiotic constraints. Root system development is tightly controlled by auxin, the driving morphogenic hormone in plants. Glutathione, a major thiol redox regulator, is also critical for root development but its interplay with auxin is scarcely understood. Previous works showed that glutathione deficiency does not alter root responses to indole acetic acid (IAA), the main active auxin in plants. Because indole butyric acid (IBA), another endogenous auxinic compound, is an important source of IAA for the control of root development, we investigated the crosstalk between glutathione and IBA during root development. We show that glutathione deficiency alters LR and RH responses to exogenous IBA but not IAA. Detailed genetic analyses suggest that glutathione regulates IBA homeostasis or conversion to IAA in the root cap. Finally, we show that both glutathione and IBA are required for the proper responses of RH to phosphate deprivation, suggesting an important role for this glutathione-dependent regulation of auxin pathway in plant developmental adaptation to its environment.

Keywords

Arabidopsis - glutathione - auxins - indole butyric acid - root system - lateral roots - root hair - phosphate

Abbreviations

IBA (indole butyric acid), IAA (indole acetic acid), LR (lateral roots), LRP (Lateral Root Primordium), RH (root hair), ROS (reactive oxygen species), GSH (reduced glutathione), GSSG (oxidised glutathione), BSO (buthionine sulfoximine), MS (Murashige and Skoog), NPA (*N*-1-naphthylphthalamic acid), NOA (1-naphthoxyacetic acid), PGPR (plant growth promoting rhizobacteria).

Accepted Manuscript

INTRODUCTION

Root developmental plasticity, combining root growth and root branching, is essential for plants to adapt and optimize their growth in changing environmental conditions, such as nutrient and water availability, rhizosphere microbiome or soil structure heterogeneity. Root growth relies on the activity of the root apical meristem that regulates histogenesis via the control of cell proliferation. Root branching is a complex organogenesis process that allows the development of new lateral roots (LR) from regularly spaced pericycle founder cells in *Arabidopsis thaliana*. These founder cells are originally specified by an oscillatory mechanism occurring in the root tip (Moreno-Risueno *et al.*, 2010; Xuan *et al.*, 2016). In addition to the root system architecture, the development of epidermal root hairs (RH) is particularly sensitive to changes in environmental conditions and contribute to the root system adaptation (Grierson *et al.*, 2014).

Among nutrients, phosphorus has a key role in all living organisms and is one of the main limiting factors for plant growth and crop productivity (Leinweber *et al.*, 2018). Its homeostasis is highly dependent on phosphate uptake by the root cap (Kanno *et al.*, 2016). Phosphate concentration strongly impacts root system development in many plant species including *Arabidopsis* (López-Bucio *et al.*, 2002, 2003; Hodge, 2004). In particular, general low phosphate availability is well known to increase RH length (Bates and Lynch, 1996). Biotic factors also modulate root development. Among them, some rhizospheric PGPR (Plant Growth Promoting Rhizobacteria) such as *Mesorhizobium loti* are able to stimulate RH elongation, hence favouring soil exploration and nutrients uptake by the plant (Vacheron *et al.*, 2013; Poitout *et al.*, 2017).

Auxins, and particularly the most abundant endogenous one, indole acetic acid (IAA), play a pivotal and integrative role in all steps of root system development, both under optimal or stress conditions (Saini *et al.*, 2013; Korver *et al.*, 2018). During LR development, auxin is responsible for the activation of founder cells, the development and organization of the LR primordia, and the emergence of the newly formed LR through the external layers of the primary root. Even earlier, the oscillatory positioning of pericycle founder cells depends on auxin maxima generated via auxin release by dying root cap cells (Moreno-Risueno *et al.*, 2010; Du and Scheres, 2018). Auxin also modulates RH elongation, thus mediating responses to stimuli such as abscisic acid or phosphate deprivation (Nacry *et al.*, 2005; Wang *et al.*, 2017). Recently, a set of works on *Arabidopsis* and rice evidenced that RH response to phosphate deprivation requires an increase in auxin *de novo* synthesis in the root cap, and its apico-basal transport to the epidermal cells via the auxin influx facilitator AUX1 (Bhosale *et al.*, 2018; Giri *et al.*, 2018; Parry, 2018).

Indole-3-butyric Acid (IBA) is a structural derivative of IAA, differing by only two additional carbons in the side chain (Korasick *et al.*, 2013). Although convincing evidence support a role for IAA in IBA biosynthesis, the mechanisms responsible and enzymes involved are still unknown (Ludwig-Müller *et al.*, 1995; Frick and Strader, 2018). It is now broadly accepted that IBA solely acts as an IAA precursor through its β -oxidative decarboxylation in peroxisomes (reviewed in Frick and Strader, 2018). This enzymatic process involves several enzymes, some shared with other β -oxidation pathways such as PED1, others apparently specific to the IBA-to-IAA conversion, such as IBR1, IBR3, IBR10 and ECH2 (Strader and Bartel, 2011; Frick and Strader, 2018). IBA homeostasis is also regulated via its transport and conjugation, but only few regulators have been identified. Type G ABC transporters ABCG36 and ABCG37 can efflux IBA from the cells (Strader and Bartel, 2009; Ruzicka *et al.*, 2010), the NPF family member TRANSPORTER OF IBA1 transports IBA across the vacuolar membrane (Michniewicz *et al.*, 2019), while the generic PXA1/COMATOSE transporter is likely to import IBA into the peroxisome. Like other auxins, IBA conjugates with sugars and amino acids. UGT84B1, UGT74D1, UGT74E2 and UGT75D1 can conjugate IBA to glucose (Jackson *et al.*, 2001; Tognetti *et al.*, 2010; Jin *et al.*, 2013; Zhang *et al.*, 2016), whereas GH3.15 is able to conjugate IBA to amino acids (Sherp *et al.*, 2018). IBA-derived IAA plays important roles during root development, including root apical meristem maintenance and adventitious rooting. IBA conversion to IAA is also critical for RH elongation (Strader *et al.*, 2010). Finally, recent works have reported the critical role of IBA-to-IAA conversion in the root cap as a source of auxin for the oscillatory positioning of LR founder cells (De Rybel *et al.*, 2012; Xuan *et al.*, 2015). IBA-to-IAA conversion taking place in the LR primordium itself also likely participates in further LR development (Strader and Bartel, 2011; Michniewicz *et al.*, 2019). Despite all these reported functions in root development, the importance of IBA-derived IAA relatively to other IAA sources is still poorly understood and scarcely documented, particularly in case of changing environmental constraints.

Changes in environmental conditions result in Reactive Oxygen Species (ROS) imbalance, thus affecting the general redox cellular homeostasis (Noctor *et al.*, 2018). For example, phosphate deficiency alters H_2O_2 and $O_2^{\cdot-}$ production in roots (Tyburski *et al.*, 2009). ROS modulate many aspects of plant development, including root system development (Singh *et al.*, 2016; Tsukagoshi, 2016). Controlled ROS production by NADPH oxidases are particularly involved in RH elongation and LR development (Carol and Dolan, 2006; Mangano *et al.*, 2016, 2018; Orman-ligeza *et al.*, 2016). Auxin and ROS pathways interact to control root development, since auxin can trigger ROS production and in turn ROS can affect IAA levels and transport (Orman-ligeza *et al.*, 2016; Tognetti, 2017; Zwiewka *et al.*, 2019).

Glutathione is a small and stable thiol-containing tripeptide (Glu-Cys-Gly) essential for plant survival and present in large concentrations in cells, up to several millimolar (Noctor *et al.*, 2012). It has many roles, including the detoxification of heavy metals and xenobiotics, sulfur homeostasis, ROS homeostasis and redox signalling. To ensure these functions, glutathione can act as a precursor (e.g. phytochelatins), be conjugated to other molecules via the Glutathione-S-transferase enzyme family, or serve as an electron donor for antioxidant systems (Noctor *et al.*, 2012). Reduced glutathione (GSH) is therefore converted to oxidised glutathione (GSSG) which is reduced back by glutathione reductases (Marty *et al.*, 2009, 2019). In standard growth conditions GSH is in large excess relative to GSSG. Glutathione biosynthesis is a 2-step reaction, with *GSH1* encoding the rate-limiting γ -glutamylcysteine synthetase and *GSH2* encoding a glutathione synthetase (Noctor *et al.*, 2012; Meyer *et al.*, 2012). Knock out mutations in any of these two genes are lethal. However, genetic screens identified several knock-down alleles of *GSH1*, allowing to get plants with reduced glutathione levels (Howden *et al.*, 1995; Vernoux *et al.*, 2000; Ball *et al.*, 2004; Parisy *et al.*, 2007; Jobe *et al.*, 2012; Shanmugam *et al.*, 2012). The importance of glutathione in root development is illustrated by the absence of root meristem maintenance in *rml1* mutant, together with the impairment of primary root growth and LR development in less severe *gsh1* alleles (Vernoux *et al.*, 2000; Bashandy *et al.*, 2010; Koprivova *et al.*, 2010; Marquez-Garcia *et al.*, 2014).

We previously reported that *cad2* or *pad2* mutants can respond almost normally to exogenous IAA for root development (Bashandy *et al.*, 2010), although auxin transport seems to be affected in glutathione-deficient plants (Bashandy *et al.*, 2010; Koprivova *et al.*, 2010). The role of glutathione in controlling root development is therefore still misunderstood. Given the importance of IBA-derived IAA in regulating root development, we chose to address the role of glutathione in root responses to IBA. We show that glutathione deficiency impairs LR and RH responses to IBA but not IAA. We then try to identify the glutathione-dependent mechanisms required for IBA responses but every IBA-related pathway examined does not reveal sensitivity to glutathione levels. We finally suggest a physiological role for this glutathione-dependent IBA response, showing that IBA and glutathione pathways are critical for RH responses to phosphate deficiency.

MATERIAL AND METHODS

Plant Material

All plants used throughout this study are in the *Arabidopsis thaliana* Col-0 ecotype. The following mutants were all previously published and available in our teams : *cad2-1* (Howden *et al.*, 1995), *pad2-1* (Parisy *et al.*, 2007), *zir1* (Shanmugam *et al.*, 2012), *gr1* (Mhamdi *et al.*, 2010), *ntra ntrb* (Bashandy *et al.*, 2010), *cat2* (Bueso *et al.*, 2007), *ibr1-2* (Zolman *et al.*, 2008), *ibr3-1* (Zolman *et al.*, 2007), *ibr10-1* (Zolman *et al.*, 2008), *ibr1 ibr3 ibr10* (Zolman *et al.*, 2008), *ech2* (Strader *et al.*, 2011), *aux1-21* (Bennett *et al.*, 1996), *pin2/eir1-1* (Roman *et al.*, 1995), *pdr8/pen3-4* (Stein *et al.*, 2006), *pdr9-2* (Ito and Gray, 2006), *ugt74e2* (Tognetti *et al.*, 2010), and *ugt74d1* (Jin *et al.*, 2013) are previously described Salk T-DNA insertion lines (Salk_000578, Salk_050885, Salk_091130 and Salk_011286, respectively) ordered from the Nottingham Arabidopsis Stock Centre (NASCC; <http://arabidopsis.info/>). The double mutants *pdr8 pdr9* and *ugt74d1 ugt74e2* were obtained by crossing the respective single mutants, and by selecting the double homozygous among F2 plants.

Plant Cultures

Seeds were surface sterilized by constant agitation with 0.05% SDS in 70% (v/v) ethanol by 20 minutes, then washed three times with ethanol 95% (v/v) and dried on sterile paper. Seeds were placed on plates containing 50 mL of ½ Murashige and Skoog medium (MS) with 0.5 g.L⁻¹ MES and 0.8 % (w/v) plant agar (Duchefa Biochemie) without sucrose unless indicated. For the experiments regarding phosphate deprivation, we used three-tenth-strength (3/10) MS supplemented with 500 µM NaCl (phosphate deprivation) or 500 µM NaH₂PO₄ (control conditions) as previously published (Arnaud *et al.*, 2014). For *Mesorhizobium loti* experiments, seeds were grown on standard ½ MS medium for 5 days, then transferred to new plates containing 0.1 OD of inoculum (Poitout *et al.*, 2017) for 4 extra days before phenotyping. All plates were incubated vertically at 20°C with 160 µE.m⁻².s⁻¹ light intensity and a 16h-light/8h-dark regime.

Phenotypic Analyses of the Root System

Lateral root density was quantified on 10-day-old seedlings by counting the number of visible lateral roots emerged and dividing by the length of the primary root section between the first and the last visible lateral roots. Lateral root primordia (LRP) density was calculated in the same way on 6-day-old seedlings using a light microscope (Axioscop2, Zeiss) for counting. For gravistimulation experiments, LRP initiation was forced by rotating the vertical plates by 90°. LRP stages were observed 48h later, using a light microscope (Axioscop2, Zeiss). For root hairs lengths quantification, plates were photographed using a camera (DFC425C, Leica) sited on a stereomicroscope (MZ12, Leica). Primary root elongation rate was quantified between day 8 and day 10. Lengths were quantified from pictures using the public domain image analysis program ImageJ 1.52i (<https://imagej.nih.gov/ij/>) and its NeuronJ plugin (Meijering *et al.*, 2004).

Glutathione Measurements

Total glutathione content of 8-day-old seedlings was determined using the recycling enzymatic assay (Rahman *et al.*, 2007). The method consists in the reduction of GSSG by glutathione reductase enzyme and NADPH to GSH. GSH levels are determined by its oxidation by 5,5'-dithio-bis(2-nitrobenzoic acid) (DTNB), that produces a yellow compound 5'-thio-2-nitrobenzoic acid (TNB), measurable at 412 nm (Rahman *et al.*, 2007). Briefly, 100 mg of fresh plant material ground in liquid nitrogen was extracted in 0.5 mL 0.1 M Na phosphate buffer, pH 7.6, and 5 mM EDTA. After micro-centrifugation (10 min, 9000g), total glutathione in 0.1 mL of the supernatant was measured by spectrophotometry in a 1 mL mixture containing 6 mM DTNB (Sigma-Aldrich), 3 mM NADPH, and 2 units of glutathione reductase from *Saccharomyces cerevisiae* (Sigma-Aldrich). Glutathione-dependent reduction of DTNB was followed at 412 nm. Total glutathione levels were calculated using the equation of the linear regression obtained from a standard GSH curve. GSSG was determined in the same extracts after derivatization of reduced GSH. Derivatization of 100 mL plant extract was performed in 0.5 mL 0.5 M K phosphate buffer, pH 7.6, in the presence of 4 mL 2-vinylpyridine (Sigma-Aldrich) during 1 h at room temperature. After extraction of the GSH-conjugated 2-vinyl pyridine with 1 volume of diethylether, GSSG was measured by spectrophotometry as described for total

glutathione.

Confocal Analyses

Auxin response analyses using *DR5:n3EGFP/DR5v2:ntdTomato* (Liao *et al.*, 2015) and the study of the redox state of glutathione with roGFP2 line (Meyer *et al.*, 2007) were performed by using a confocal laser scanning microscope LSM 700 (Zeiss). Images were acquired in 16-bits using a 10x EC Plan Neofluar objective (Zeiss). Settings were based on the respective methods previously published (Meyer *et al.*, 2007; Liao *et al.*, 2015) with minor modifications. Excitation of roGFP2 was performed at 488 and 405 nm and a bandpass (BP 490-555 nm) emission filter was used to collect roGFP2 signal. For background subtraction, signal was recovered using a BP 420-480 nm emission filter during excitation at 405 nm.

For *DR5:n3EGFP/DR5v2:ntdTomato* analysis, seeds were grown on standard ½ MS medium supplemented or not with BSO 0.5mM (pre-treatment). 7-day-old seedlings were transferred for 24 hours to plates containing the appropriate treatments (IBA 10µM, IAA 50nM), still combined or not with BSO 0.5mM, according to the pre-treatment. Regarding the analyses with roGFP2, seeds were grown for 8 days in ½ MS medium containing or not IBA 10µM.

Pictures analyses and quantifications were performed as previously described for both probes (Meyer *et al.*, 2007; Liao *et al.*, 2015), using the public domain image analysis program ImageJ 1.52i (<https://imagej.nih.gov/ij/>).

Histochemical Localization of GUS Activity

Plants were fixed in 80% (v/v) acetone at 20 °C for 20 minutes, then washed with buffer solution, containing 25 mM Na₂HPO₄, 25mM NaH₂PO₄, 2% Triton X-100 (v/v), 1 mM K₃Fe(CN)₆, and 1 mM K₄Fe(CN)₆. Thereafter, staining was performed at 37 °C in the buffer solution containing 2mM of X-Gluc (5-bromo-4-chloro-3-indolyl-β-D-glucuronidase) as substrate (Jefferson *et al.*, 1987), after 1 min vacuum infiltration. The reaction was stopped by changing the seedlings to ethanol 70% (v/v). Pictures were collected using a light microscope (Axioscop2, Zeiss).

Gene Expression Quantification

Total RNA was extracted using TriZol reagent (GE Healthcare, UK), and the RNA was purified with RNeasy Plant Mini Kit (Promega, USA), according to the manufacturer protocols. cDNA was subsequently synthesized using the GoScript™ Reverse Transcription System (Promega, USA). Quantitative real-time PCR was done using Takyon™ No Rox SYBR® MasterMix blue dTTP (Eurogentec, Belgium) and the LightCycler 480 (Roche, Switzerland). Primers used are presented in Supplementary Table 1. All reported results are presented normalized with the *ACTIN2* control gene but behave similarly if normalized with *ACTIN7* or *GAPDH* control genes.

Auxin Accumulation Assays

5-mm root tips from 8-day-old seedlings were excised and incubated in 40 µL uptake buffer (20 mM MES, 10 mM sucrose, and 0.5 mM CaSO₄, pH 5.6) for 15 min at room temperature. Root tips were then incubated for one hour in uptake buffer containing 25 nM [³H]-IAA (20 Ci/mmol; American Radiolabeled Chemicals) or [³H]-IBA (25 Ci/mmol; American Radiolabeled Chemicals) prior to washing with three changes of uptake buffer. Root tips were then placed in 3 mL CytoScint-ES liquid scintillation cocktail (MP Biomedicals) and analyzed by scintillation counting.

Data Replicability and Statistical Analyses

All the presented experiments illustrate results obtained in at least three independent biological repetitions. For *in vitro* phenotyping experiments, each biological repetition consisted in two technical replicate plates per condition, each containing around 12 seeds for the mutant and 12 for the appropriate control, sown side by side. Statistical analyses were performed as indicated in Figure legends.

Accession Numbers

Sequences from this article can be found in the Arabidopsis Genome Initiative database under the following accession numbers : *GSH1* (*At4g23100*), *GR1* (*At3g24170*), *NTRA* (*At2g17420*), *NTRB* (*At4g35460*), *CAT2* (*At4g35090*), *AUX1* (*At2g38120*), *PIN2* (*At5g57090*), *PDR8/PEN3* (*At1g59870*), *PDR9* (*At3g53480*),

UGT74D1 (At2g31750), *UGT74E2* (At1g05680), *IBR1* (At4g05530), *IBR3* (At3g06810), *IBR10* (At4g14430), *ECH2* (At1g76150), *AIM1* (At4g29010), *PED1* (At2g33150), *PHT1;4* (At2g38940), *RNS1* (At2g02990), *SPX1* (At5g20150), *ACT2* (At3g18780).

RESULTS

Glutathione deficiency specifically alters LR and RH responses to IBA but not IAA

Since IBA plays important roles during root development, we investigated root responses to both IAA and IBA in several *gsh1* weak alleles and in plants treated with Buthionine Sulfoximine (BSO), a chemical specific inhibitor of GSH1 enzyme.

We first wanted to precisely know the glutathione levels in the different genotypes in our growth conditions, thus we quantified endogenous glutathione in whole 8-day old seedlings (Figure 1A). We find the same amount of total glutathione (*i.e.* about 25% of wild-type content) in *cad2* and *pad2* mutants, which was expected. We show that 1mM exogenous BSO also reduces endogenous glutathione levels of wild type plants to approximately the same levels. In addition, we report that exogenous IBA treatment does not impact endogenous glutathione levels.

Supplementary Figures 1A and 1B show that *cad2* and *pad2* mutants display the same primary root growth as the wild-type in our growth conditions, and that the primary root responds normally to both IAA and IBA. In the same way, BSO treatment (1mM) neither affects primary root growth nor its response to IAA or IBA.

As expected, both IAA and IBA also induce LR density in the mature zone of the root in 10-day-old seedlings (Figure 1B). LR density in both *cad2* and *pad2* mutants responds normally to IAA treatment but displays hyposensitivity to exogenous IBA. As expected, the addition of BSO phenocopies *cad2* and *pad2* mutants (Supplementary Figure 2A). Finally, we could revert *cad2* hyposensitivity to IBA by adding exogenous GSH, while it has no effect on wild-type plants sensitivity to IBA (Supplementary Figure 2B). Because final emerged LR density depends both on LR initiation and subsequent LRP development, we also addressed the LRP density in the same conditions. Figure 1C reveals that both LRP and emerged LR densities display IBA hyposensitivity in plants with low glutathione levels, suggesting that glutathione affects LR development upstream of LRP development. Another way to

investigate LRP development is to force and synchronize LRP initiation by gravistimulation (Péret *et al.*, 2012). We therefore gravistimulated glutathione-deficient plants, in the absence or presence of exogenous IBA (10 μ M). We observe that exogenous IBA treatment slightly slows down wild-type LRP development upon gravistimulation in our growth conditions (Figure 1D). We also observe that *cad2*, *pad2* and BSO-treated plants respond to IBA in a similar way as wild-type. This suggests that, once established, the LRP development regulation by IBA is independent of glutathione, at least in its later stages. Taken together, these results tend to support a role for glutathione in IBA-dependent specification or activation of founder cells necessary for the initial establishment of LRP.

Finally, we monitored RH elongation responses to IBA and IAA in glutathione-deficient plants (Figure 1E and 1F). As for LR, we notice that *cad2* and *pad2* mutants are hyposensitive to the IBA-dependent induction of RH growth but respond normally to IAA. Similarly, 1 mM BSO treatment also reduces the RH response to IBA but not IAA. We can therefore conclude that glutathione is also required for the IBA-dependent induction of RH growth.

Glutathione levels affect auxin signalling in the basal part of the meristem.

We have shown that glutathione deficiency alters RH elongation and LRP density in response to IBA. We know that root tip-derived IAA transits through the lateral root cap to regulate both founder cell positioning and RH growth in the basal part of the meristem. We therefore investigated auxin response in the root tip, by using the *DR5:GUS* auxin signalling reporter (Ulmasov *et al.*, 1997). In standard growth conditions, we only reveal GUS staining in the quiescent center and the columella, and BSO treatment by itself does not change the *DR5:GUS* expression pattern (Figure 2A). As expected, exogenous IAA treatment for 24 hours induces auxin response in the whole root tip and root epidermis, and the presence of BSO has again no effect on this distribution. In response to IBA, GUS staining increases in the distal meristem and strongly appears specifically in the trichoblast epidermal cell files in the basal part of the meristem, up to the differentiation zones. In the presence of BSO, this IBA-dependent strong signal in the basal meristem almost disappears while the signal in the distal meristem remains strong.

In order to confirm these results, we used another auxin signalling marker that allows the quantification of auxin response, the *DR5:n3EGFP/DR5v2:ntdTomato* double reporter line (Liao *et al.*, 2015). We quantified both GFP and Tomato fluorescence in the distal and basal parts of the meristem (Figure 2B). In agreement with the *DR5:GUS* reporter line, both IBA and IAA treatments increase auxin signalling in distal and basal parts of the meristem. The presence of BSO does not significantly alter auxin signalling, neither in standard conditions nor upon exogenous IAA treatment.

However, we can confirm that BSO severely represses IAA signalling in the basal part of the meristem in response to exogenous IBA, while it has limited effect in the distal part.

Hence we show that glutathione is specifically required for IBA-derived IAA signalling in the basal part of the meristem, where LR founder cells are specified and RH growth is determined. Moreover, we show that glutathione does not affect IAA signalling components since auxin signalling reporters respond normally to exogenous IAA when glutathione content is depleted.

IBA-derived IAA responses are specifically affected by glutathione deficiency

Because glutathione is a critical regulator of cellular redox homeostasis, we addressed root responses to IBA in other redox-related mutants. We chose to analyse the *gr1* mutant, affected in cytosolic and peroxisomal glutathione reduction (Marty *et al.*, 2009), the *cat2* mutant, affected in H₂O₂ detoxification (Queval *et al.*, 2007), and the *ntra ntrb* double mutant affected in the thioredoxin-dependent thiols reduction system (Reichheld *et al.*, 2007). Quantification of both GSH and GSSG (Figure 3A) shows that *gr1*, *ntra ntrb* and *cat2* mutant plants have higher total glutathione concentrations than wild type plants. The application of exogenous IBA has almost no effect on both GSH and GSSG levels. As expected, *cat2* and *gr1* mutants also display higher glutathione oxidation status. In addition, the use of the roGFP2 probe allowed us to confirm that the presence of IBA does not generate any imbalance in glutathione redox status in root tissues (Figure 3B and Supplementary Figure 3). In contrast to *cad2*, none of the other mutants display any LR density hyposensitivity to IBA (Figure 3C). These results suggest that root responses to IBA specifically depend on glutathione overall levels rather than glutathione redox status or any general redox imbalance.

IAA transport from the distal to the basal meristem is not targeted by glutathione

We have presented data showing that the IBA-derived IAA response in the basal meristem is dependent on glutathione levels. AUX1 and PIN2 are the IAA transporters that ensure the apico-basal IAA flux in the root cap and the root tip epidermis. We previously published that strong BSO treatment induces long-term decrease in the expression of *AUX1* and *PIN2* (Bashandy *et al.*, 2010).

In order to determine if *AUX1* and/or *PIN2* are the targets of glutathione to modulate root responses to IBA, we examined LR density in *aux1* and *pin2* mutants. As shown in Figure 4A, *aux1* and *pin2* mutants still display hyposensitivity to IBA upon BSO treatment. In other words, the glutathione regulation still occurs in both *aux1* and *pin2* mutants, revealing that neither AUX1 nor PIN2 is regulated by glutathione to control root responses to IBA. Because AUX1 and PIN2 are members of multigene families, we wanted to ensure that other members of AUX/LAX or PIN families are not replacing AUX1 and PIN2 in the respective mutants. We therefore addressed IBA responses with or

without BSO treatment in the presence of specific inhibitors of both families (Figure 4B). We observed that BSO still leads to LR hyposensitivity to IBA both in the presence of *N*-1-naphthylphthalamic acid (NPA), that inhibits PIN-dependent auxin efflux, and 1-naphthoxyacetic acid (NOA), a specific inhibitor of AUX/LAX influx facilitators. All together these data suggest that the glutathione-dependent control of root responses to IBA does not affect IAA transport from the root apex to the basal meristem.

Looking for glutathione targets in IBA pathways.

Since IAA transport was not the target of glutathione, we investigated IBA homeostasis in plants with low glutathione content. Interestingly, *gsh1* mutants display pleiotropic phenotypes opposite to the phenotypes of mutant alleles in *PDR8/PEN3/ABCG36* for IBA sensitivity, but also for sensitivity to *Pseudomonas* and cadmium treatments (Kim *et al.*, 2007; Strader and Bartel, 2009; Lu *et al.*, 2015). ABCG36, together with its homolog PDR9/ABCG37, is responsible for IBA efflux from the cells, which prompted us to investigate the IBA import into plant cells in the *cad2* mutant. As shown in Figure 5A, we did not detect any impairment in ³H-IBA accumulation in *cad2* excised root tips, in contrast with the expected reduction of uptake in a gain-of-function allele of *PDR9* (*pdr9-1*). This suggests that IBA uptake from the medium is not perturbed by glutathione deficiency. This is consistent with the normal response of primary root growth to IBA in such conditions (Supplementary Figures 1A and 1B).

In order to better investigate IBA transport, we analysed the glutathione-dependent LR and RH response to IBA in *abcg36/pdr8* and *abcg37/pdr9* mutants (Figure 5B and Supplementary Figure 4). As expected, *pdr8* mutant displays hypersensitivity to exogenous IBA. However, both mutants are still clearly resistant to IBA in the presence of BSO. Because of putative redundancy between these two proteins, we generated the *pdr8 pdr9* double mutant that displays a *pdr8*-like hypersensitivity of LR density to exogenous IBA. As for single mutants, LR density and RH length in the double mutant are induced by IBA but BSO is still able to decrease this response. This result means that IBA efflux transporters ABCG36 and ABCG37 are not the targets of glutathione-dependent regulation.

We know that IBA homeostasis is also regulated via conjugation with glucose, and several glycosyltransferases are able to catalyse such a reaction (Jackson *et al.*, 2001; Tognetti *et al.*, 2010; Jin *et al.*, 2013; Zhang *et al.*, 2016). Among them, we assayed *ugt74d1* and *ugt74e2* mutants. Again, we could observe that LR and RH responses to IBA are still BSO-sensitive in both mutants, although *ugt74d1* LR density is hypersensitive to IBA compared to wild-type (Figure 5C and Supplementary Figure 4). Because of putative redundancy between these two glycosyltransferases, we generated an

ugt74e2 ugt74d1 double mutant. However, the response to IBA is still reduced in the presence of BSO in the double mutant, suggesting that these glycosyltransferases are not the targets of glutathione-dependent regulation.

Finally, we also investigated the enzymatic pathway involved in the IBA-to-IAA conversion in the peroxisome. Figure 6A shows that *ibr1*, *ibr10* and *ibr1 ibr3 ibr10* mutants are fully insensitive to exogenous IBA in our growth conditions, thus making impossible to genetically address the putative dependency of IBR1 and IBR10 to glutathione levels. However, we noticed that in *ech2* and *ibr3* mutants, LR are still hyposensitive to IBA in the presence of BSO. Again, this suggests that ECH2 and IBR3 are not regulated in a glutathione-dependent manner. In order to detect an eventual defect in gene expression in glutathione-deficient plants, we analysed the expression level of genes involved in IBA-to-IAA conversion (Figure 6B). Surprisingly, *ECH2*, *IBR1*, *IBR3*, *IBR10*, *AIM1* and *PED1* genes were all moderately (10 to 50 % increase) but consistently upregulated in *cad2* mutant compared to the wild-type. In any case, this does not allow us to identify any target that could be transcriptionally down-regulated upon glutathione depletion.

To conclude, we carefully examined most of the known components of IBA homeostasis and response pathways, but none of them seem to be the target of glutathione-dependent regulation.

IBA and glutathione control RH responses to phosphate deprivation

We analysed RH elongation rate in response to phosphate starvation and to *Mesorhizobium loti* (*M. loti*). We observed that both stimuli increase RH length in wild-type plants (Figure 7, A and B). Both *cad2* and *ibr1 ibr3 ibr10* mutants display wild-type like RH response to *M. loti*, suggesting that neither glutathione nor IBA participate in RH elongation response to PGPR (Figure 7A).

In contrast we observed that *cad2* mutant is clearly hyposensitive to phosphate deprivation, and that RH elongation response to phosphate starvation is almost fully abolished in *ibr1 ibr3 ibr10* mutant (Figure 7B). We also confirmed the decreased glutathione levels in *cad2* mutant while *ibr1 ibr3 ibr10* mutant does not alter glutathione content and redox status (Supplementary Figure 5). Interestingly, phosphate deprivation does not significantly affect total glutathione content in plants but increases the GSH/GSSG ratio.

We wondered if *cad2* and *ibr1 ibr3 ibr10* mutants affect the general response to phosphate deficiency or specifically the response of root hairs to this abiotic stress. We therefore quantified the expression of marker genes known to be induced in response to phosphate deprivation. Figure 7C shows that the induction of the expression of marker genes in response to phosphate starvation is not abolished in *cad2* and *ibr1 ibr3 ibr10* mutants. We only noticed a slight down-regulation of *SPX1*

in *cad2* mutant. As *SPX1* encodes a negative regulator of phosphate starvation responses, this could explain why other responsive genes are slightly up-regulated in *cad2*.

We can conclude that both IBA conversion to IAA and glutathione are required for proper root hair response to phosphate starvation, without affecting general responses to this abiotic stress.

DISCUSSION

Glutathione regulation of IBA homeostasis or conversion to IAA in the root cap

In this work, we first report that root hair and lateral root responses to exogenous IBA, but not IAA, are impaired by glutathione deficiency. More precisely, the glutathione-dependent control of IBA response affects early steps of LR development, either founder cells specification or their activation to divide and form a LR primordium. We also show that low glutathione levels alter IBA-dependent auxin signalling in the basal meristem, where RH elongation occurs and LR founder cells are specified. Finally, we show in this manuscript that transporters known to be involved in the apico-basal flux of IAA to the basal meristem, namely *AUX1* and *PIN2*, are not the targets of the glutathione-dependent control. All these data strongly suggest that glutathione modulates IBA homeostasis or IBA-to-IAA conversion in the root cap, although it does not exclude that the same regulation can also occur in additional tissues.

All the phenotypes reported here concern root responses to exogenous IBA and one can wonder if the glutathione-dependent regulation normally occurs in physiological conditions, modulating pathways relying on endogenous IBA. Because of our scarce knowledge of IBA metabolism and the absence of genetic tools concerning IBA biosynthesis, it is rather difficult to address such question. However, we accumulated several clues that, taken together, strongly support the importance of glutathione for the control of endogenous IBA pathways. First, we observe in *cad2* mutant seedlings grown under standard conditions (*i.e.* without exogenous IBA) a general increase in the expression of all genes involved in IBA-to-IAA conversion (Figure 6B). This might reveal a feedback mechanism that would report an excess of IBA or a depletion in IBA-derived IAA in low glutathione conditions. Secondly, we observe that both *ugt* and *pdr* double mutants are hypersensitive to exogenous IBA (Figures 5B and 5C), which is consistent with the already reported overaccumulation of endogenous free IBA in corresponding single mutants (Strader and Bartel, 2009; Tognetti *et al.*, 2010; Ruzicka *et al.*, 2010). Interestingly, it looks like BSO has more effect in both *ugt* and *pdr* mutant genotypes than for the wild-type plants, reducing IBA response by 20 to 25% in wild type plants, but by 28 to 33% in *pdr* and *ugt* double mutants, respectively (Figures 5B and 5C). This supports a role for glutathione in

modulating responses to endogenous IBA. Finally, we show that both *cad2* and *ibr1 ibr3 ibr10* triple mutant display hyposensitivity in their RH response to phosphate, but not to *Mesorhizobium loti*. In addition, both are not impaired in the general plant response to phosphate deprivation, but only in the RH elongation response. This set of arguments proves that both endogenous IBA pathway and glutathione mediate RH response to phosphate starvation, and strongly suggests that the glutathione-dependent regulation of endogenous IBA pathway is modulating the RH response.

Auxins fine-tuning of root architecture in response to phosphate availability

Although well-known to play important roles in plant development, the function of IBA as a source of IAA relative to other IAA sources, such as *de novo* synthesis or conjugated forms, is still very mysterious and we might wonder “Why plants need more than one type of auxins?” (Simon and Petrášek, 2011; Frick and Strader, 2018). A previous work has reported that IBA regulates both plant development and resistance to water stress, suggesting an important function for IBA in adapting plant development to abiotic stress (Tognetti *et al.*, 2010). However, to our knowledge, our work is the first to clearly demonstrate that IBA-dependent pathway is necessary for IAA to adapt some developmental pathway, *i.e.* root hair elongation, to a specific abiotic stress (phosphate starvation).

In their recent work, Bhosale *et al.* (2018) already revealed the increase in IAA levels in the root cap in response to low external phosphate, necessary for RH elongation. However, because they observe a significant increase in *TAA1* (*TRYPTOPHAN AMINOTRANSFERASE OF ARABIDOPSIS 1*) gene expression in such conditions, they hypothesized that the increase in IAA levels in the root cap is due to the induction of Indole-3-Pyruvic Acid (IPyA)-dependent pathway, the main one responsible for *de novo* IAA synthesis in Arabidopsis (Mashiguchi *et al.*, 2011). Intriguingly, RH elongation response to external low phosphate is almost completely abolished in both *ibr1 ibr3 ibr10* and *taa1* mutants (Figure 7B and Bhosale *et al.*, 2018: Figures 2b and 2c). One could imagine that two independent routes of IAA synthesis, *i.e.* the *TAA1*-dependent *de novo* synthesis and the IBA-to-IAA conversion, are both critical and induced in the root cap in response to phosphate deprivation. IBA can itself be derived from IAA and we can imagine that an increase in IBA-to-IAA conversion would require an increase in IBA levels, and therefore more IAA to supply the IBA stock. However, thinking to a root cap increase in IAA to increase IBA in order to increase IAA gets almost no sense. Thus, we suggest that external low phosphate induces *TAA1* expression in the whole plant to increase global available auxin levels on the one hand, and in the other hand activates the local IBA-to-IAA conversion in the root cap to ensure a local appropriate developmental response.

However, we must remind that we are working *in vitro* with homogenous media containing a given concentration of phosphate. A very elegant recent work has reported that, when subjected to a heterogenous environment, using a Dual-flow-root chip, a single root increases RH length in the medium having the highest phosphate concentration (Stanley *et al.*, 2018). This observation contrasts with the induction of RH growth by low phosphate in homogenous *in vitro* media. RH adaptation to phosphate probably results from the crosstalk between a systemic information based on overall available phosphorus in the plant, and a local information based on phosphate availability in the environment, that we cannot differentiate in our *in vitro* homogenous conditions. Such dual control has been extensively documented for root responses to another important nutrient, nitrogen (Ruffel and Gojon, 2017). We might therefore envisage that both sources of IAA are differentially regulated by systemic and local signals. This might ensure a very acute dosage of free IAA to optimize root adaptation to the plant metabolism and environment. In such context, glutathione could be a central regulator of local IBA-to-IAA adaptation to external phosphate in the root cap.

Unravelling the glutathione-dependent regulation of IBA pathway

Although we explored most of known components of IBA pathways (Supplementary Figure 6), we were not able to identify how glutathione regulates IBA homeostasis or conversion to IAA. This can first be explained by the difficulties to work with IBA which is present in low amounts compared to IAA in plants, and is therefore difficult to detect and quantify (Frick and Strader, 2018). Moreover, many components of the IBA pathways remain to be identified. For sure, the development of new tools, such as IBA-specific reporters or probes, or mutants in IBA biosynthesis, would be very helpful to depict the important roles played by this auxin in plants. The other problem we faced is the complex multifaceted roles of glutathione in cells, that prevented us to try to decipher the mechanism from the glutathione starting point. The only clue we get is that IBA hyposensitivity is specific to plants with reduced amounts of glutathione but does not occur in plants affected in other redox pathways like glutathione or thioredoxin reduction (Figure 3). This suggests that IBA regulation by glutathione may act through glutathionylation or via the activity of thiols reductases that specifically depend on glutathione, such as glutaredoxins. One hypothesis would be that IBA, or a precursor, could itself be glutathionylated, which would be responsible for its storage or transport. In Arabidopsis, the Tau class of Glutathione-S-Transferases (GSTU) have been shown to glutathionylate some fatty acids, ranging from short to long acyl chains (Dixon and Edwards, 2009). Similarly, GSTU19 and GSTF8 have been proposed to glutathionylate 12-oxo-phytodienoic acid (OPDA), hence allowing its translocation from the chloroplast to the peroxisome where it is

converted to Jasmonic Acid (Davoine, 2006; Dixon and Edwards, 2009). Interestingly, among the 28 members of the Tau class, encoding cytosolic enzymes, several *GSTU* genes are transcriptionally regulated by IBA in the Arabidopsis root tip (Xuan *et al.*, 2015) and/or by phosphate deficiency in Arabidopsis roots (Lin *et al.*, 2011) and could be good candidates. It would be interesting to assay the IBA responses of RH and LR in corresponding mutants.

Because IBA-to-IAA conversion occurs in the peroxisome, we might also envisage that the glutathione-dependent regulation is not specific to IBA pathways but affects the peroxisomal machinery. One of the main peroxisomal functions is the β -oxidation of fatty acids, which is essential to supply energy during seed germination. We never observed any defect in seed germination in *cad2* or *pad2* mutants, in contrast to mutants in peroxisomal functions which generally strongly affect seed germination. However, we cannot exclude that the glutathione-dependent regulation only occurs in the root cap and therefore mainly affects IBA-to-IAA conversion although regulating the peroxisome machinery. Among the PEROXINS proteins, many participate in the peroxisomal matrix protein import machinery (Cross *et al.*, 2016). PEX5 is a central cargo protein that recognizes proteins targeted with the specific PTS1 (Peroxisomal Targeting Signal 1) signal peptide and import them into the peroxisome. PEX7 recognizes proteins harbouring another signal peptide (PTS2), and then binds to PEX5 for import into the peroxisome. Interestingly, previous works on human and *Pichia pastoris* PEX5 revealed that its activity and oligomerization depend on a redox switch affecting a conserved N-terminal cysteine (Ma *et al.*, 2013; Apanasets *et al.*, 2014). However, such regulation is not specific to glutathione but rather depends on the redox status and the content in ROS of peroxisomes.

Finally, the last hypothesis would be that glutathione regulates IBA homeostasis or conversion to IAA via a yet unidentified or not assayed component. Quantification of IBA-to-IAA conversion would be helpful in order to confirm this hypothesis. Concerning the IBA-to-IAA β -oxidation pathway in the peroxisome, PED1 has been reported to harbour a redox-sensitive switch affecting a conserved cysteine and that participates in activating the enzyme when reduced (Pye *et al.*, 2010). In contrast to most of the other enzymes involved in the conversion pathway, PED1 is targeted to the peroxisome through a PTS2 signal peptide. It is interesting to notice that *pex5-1*, in contrast to *pex5-10*, is not altered in PTS1-dependent import but only in PTS2-dependent import of proteins into the peroxisome (Woodward and Bartel, 2004; Khan and Zolman, 2010). *pex5-1*, although not displaying any phenotype during germination, is highly affected in IBA responses. This might reveal that IBA to IAA conversion is highly dependent on a PTS2-targeted protein, and PED1 could therefore be a good candidate to assay. However, PED1 is not specific to IBA-to-IAA pathway since it acts in almost all β -

oxidation pathways occurring in the peroxisome. We could imagine a local glutathione-dependent regulation of PED1 activity specifically in the root cap.

In conclusion, our work points out the important role of glutathione in both controlling IBA-to-IAA conversion required for proper root development and mediating developmental responses to nutrient deprivation. This opens novel perspectives in understanding how redox homeostasis can signal and integrate environmental constraints to trigger proper developmental adaptations via the regulation of morphogenetic hormonal pathways.

Accepted Manuscript

ACKNOWLEDGMENTS

We thank Edouard Jobet for his technical support for qPCR experiments. We thank the “Bio-Environnement” technological UPVD platform (Région Occitanie, CPER 2007-2013 Technoviv, CPER 2015-2020 Technoviv2), for access to the confocal microscope and qPCR facilities. This work was supported by the Agropolis Foundation (Flagship project CalClim), the Centre National de la Recherche Scientifique and the Université de Perpignan Via Domitia. This study is set within the framework of the "Laboratoires d'Excellence (LabEx)" TULIP (ANR-10-LABX-41). JA T-H is supported by a PhD grant from “Consejo Nacional de Ciencia y Tecnología” (CONACYT:254639/411761).

Accepted Manuscript

REFERENCES

- Apanasets O, Grou CP, Van Veldhoven PP, Brees C, Wang B, Nordgren M, Dodt G, Azevedo JE, Fransen M.** 2014. PEX5, the Shuttling Import Receptor for Peroxisomal Matrix Proteins, Is a Redox-Sensitive Protein. *Traffic* **15**, 94–103.
- Arnaud C, Clement M, Thibaud M-C, et al.** 2014. Identification of Phosphatin, a Drug Alleviating Phosphate Starvation Responses in Arabidopsis. *Plant Physiology* **166**, 1479–1491.
- Ball L, Accotto G-P, Bechtold U, et al.** 2004. Evidence for a Direct Link between Glutathione Biosynthesis and Stress Defense Gene Expression in Arabidopsis. *The Plant Cell* **16**, 2448–2462.
- Bashandy T, Guillemint J, Vernoux T, Caparros-Ruiz D, Ljung K, Meyer Y, Reichheld J-P.** 2010. Interplay between the NADP-linked thioredoxin and glutathione systems in Arabidopsis auxin signaling. *The Plant cell* **22**, 376–91.
- Bates TR, Lynch JP.** 1996. Stimulation of root hair elongation in Arabidopsis thaliana by low phosphorus availability. *Plant, Cell and Environment* **19**, 529–538.
- Bennett MJ, Marchant A, Green HG, May ST, Ward SP, Millner PA, Walker AR, Schulz B, Feldmann KA.** 1996. Arabidopsis AUX1 Gene: A Permease-Like Regulator of Root Gravitropism. *Science* **273**, 948–950.
- Bhosale R, Giri J, Pandey BK, et al.** 2018. A mechanistic framework for auxin dependent Arabidopsis root hair elongation to low external phosphate. *Nature Communications* **9**, 1–9.
- Bueso E, Alejandro S, Carbonell P, Perez-Amador MA, Fayos J, Bellés JM, Rodriguez PL, Serrano R.** 2007. The lithium tolerance of the Arabidopsis cat2 mutant reveals a cross-talk between oxidative stress and ethylene. *Plant Journal* **52**, 1052–1065.
- Carol RJ, Dolan L.** 2006. The role of reactive oxygen species in cell growth : lessons from root hairs. *Journal of Experimental Botany* **57**, 1829–1834.
- Cross LL, Ebeed HT, Baker A.** 2016. Peroxisome biogenesis, protein targeting mechanisms and PEX gene functions in plants. *Biochimica et Biophysica Acta - Molecular Cell Research* **1863**, 850–862.
- Davoine C.** 2006. Adducts of Oxylipin Electrophiles to Glutathione Reflect a 13 Specificity of the Downstream Lipoxygenase Pathway in the Tobacco Hypersensitive Response. *Plant Physiology* **140**, 1484–1493.
- Dixon DP, Edwards R.** 2009. Selective binding of glutathione conjugates of fatty acid derivatives by plant glutathione transferases. *Journal of Biological Chemistry* **284**, 21249–21256.
- Du Y, Scheres B.** 2018. Lateral root formation and the multiple roles of auxin. *Journal of Experimental Botany* **69**, 155–167.
- Frick EM, Strader LC.** 2018. Roles for IBA-derived auxin in plant development. *Journal of Experimental Botany* **69**, 169–177.
- Giri J, Bhosale R, Huang G, et al.** 2018. Rice auxin influx carrier OsAUX1 facilitates root hair elongation in response to low external phosphate. *Nature Communications* **9**, 1408.
- Grierson CS, Nielsen E, Ketelaar T, Schiefelbein J.** 2014. Root Hairs. *The Arabidopsis Book*.e0172.
- Hodge A.** 2004. The plastic plant: Root responses to heterogeneous supplies of nutrients. *New Phytologist* **162**, 9–24.
- Howden R, Andersen CR, Coldsbrough B, Cobbett CS.** 1995. A Cadmium-Sensitive, Glutathione-Deficient

Mutant of *Arabidopsis thaliana*. *Plant Physiology* **107**, 1067–1073.

Ito H, Gray WM. 2006. A Gain-of-Function Mutation in the *Arabidopsis* Pleiotropic Drug Resistance Transporter PDR9 Confers Resistance to Auxinic Herbicides. *Plant Physiology* **142**, 63–74.

Jackson RG, Lim EK, Li Y, Kowalczyk M, Sandberg G, Hogget J, Ashford DA, Bowles DJ. 2001. Identification and Biochemical Characterization of an *Arabidopsis* Indole-3-acetic Acid Glucosyltransferase. *Journal of Biological Chemistry* **276**, 4350–4356.

Jefferson RA, Kavanagh TA, Bevan MW. 1987. GUS fusions: beta-glucuronidase as a sensitive and versatile gene fusion marker in higher plants. *The EMBO journal* **6**, 3901–3907.

Jin SH, Ma XM, Han P, Wang B, Sun YG, Zhang GZ, Li YJ, Hou BK. 2013. UGT74D1 Is a Novel Auxin Glucosyltransferase from *Arabidopsis thaliana*. *PLoS ONE* **8**, e61705.

Jobe TO, Sung D-Y, Akmakjian G, Pham A, Komives EA, Mendoza-Cózatl DG, Schroeder JI. 2012. Feedback inhibition by thiols outranks glutathione depletion : a luciferase-based screen reveals glutathione-deficient c -ECS and glutathione synthetase mutants impaired in cadmium- induced sulfate assimilation. *The Plant Journal* **70**, 783–795.

Kanno S, Pe B, Berthome R, Bayle V, Delannoy E, Marin E, Nakanishi TM. 2016. A novel role for the root cap in phosphate uptake and homeostasis. *eLIFE*, 1–16.

Khan BR, Zolman BK. 2010. pex5 Mutants That Differentially Disrupt PTS1 and PTS2 Peroxisomal Matrix Protein Import in *Arabidopsis*. *Plant Physiology* **154**, 1602–1615.

Kim DY, Bovet L, Maeshima M, Martinoia E, Lee Y. 2007. The ABC transporter AtPDR8 is a cadmium extrusion pump conferring heavy metal resistance. *Plant Journal* **50**, 207–218.

Koprivova A, Mugford ST, Kopriva S. 2010. *Arabidopsis* root growth dependence on glutathione is linked to auxin transport. *Plant cell reports* **29**, 1157–67.

Korasick DA, Enders TA, Strader LC. 2013. Auxin biosynthesis and storage forms. *Journal of Experimental Botany* **64**, 2541–2555.

Korver RA, Koevoets IT, Testerink C. 2018. Out of Shape During Stress : A Key Role for Auxin. *Trends in Plant Science* **23**, 783–793.

Leinweber P, Bathmann U, Buczko U, et al. 2018. Handling the phosphorus paradox in agriculture and natural ecosystems: Scarcity, necessity, and burden of P. *Ambio* **47**, 3–19.

Liao C, Smet W, Brunoud G, Yoshida S, Vernoux T, Weijers D. 2015. Reporters for sensitive and quantitative measurement of auxin response. *Nature Methods* **12**, 207–210.

Lin WD, Liao YY, Yang TJW, Pan CY, Buckhout TJ, Schmidt W. 2011. Coexpression-based clustering of *Arabidopsis* root genes predicts functional modules in early phosphate deficiency signaling. *Plant Physiology* **155**, 1383–1402.

López-Bucio J, Cruz-Ramírez A, Herrera-Estrella L. 2003. The role of nutrient availability in regulating root architecture. *Current Opinion in Plant Biology* **6**, 280–287.

López-Bucio J, Hernandez-Abreu E, Sanchez-Calderon L, Nieto-jacobo F, Simpson J, Herrera-estrella L. 2002. Phosphate Availability Alters Architecture and Causes Changes in Hormone Sensitivity in the *Arabidopsis*. *Plant Physiology* **129**, 244–256.

Lu X, Dittgen J, Piślewska-Bednarek M, et al. 2015. Mutant Allele-Specific Uncoupling of PENETRATION3 Functions Reveals Engagement of the ATP-Binding Cassette Transporter in Distinct Tryptophan Metabolic

Pathways. *Plant Physiology* **168**, 814–827.

Ludwig-Müller J, Hilgenberg W, Epstein E. 1995. THE IN VITRO BIOSYNTHESIS OF INDOLE-3-BUTYRIC ACID IN MAIZE. *Phytochemistry* **40**, 61–68.

Ma C, Hagstrom D, Polley SG, Subramani S. 2013. Redox-regulated cargo binding and release by the peroxisomal targeting signal receptor, Pex5. *Journal of Biological Chemistry* **288**, 27220–27231.

Mangano S, Denita-juarez SP, Marzol E, Borassi C, Estevez JM. 2018. High Auxin and High Phosphate Impact on RSL2 Expression and ROS-Homeostasis Linked to Root Hair Growth in *Arabidopsis thaliana*. *Frontiers in Plant Science* **9**, 1164.

Mangano S, Paola S, Juárez D, Estevez JM. 2016. Update on Polar Growth ROS Regulation of Polar Growth in Plant Cells. *Plant Physiology* **171**, 1593–1605.

Marquez-Garcia B, Njo M, Beeckman T, Goormachtig S, Foyer CH. 2014. A new role for glutathione in the regulation of root architecture linked to strigolactones. *Plant, cell & environment* **37**, 488–98.

Marty L, Bausewein D, Müller C, et al. 2019. *Arabidopsis* glutathione reductase 2 is indispensable in plastids, while mitochondrial glutathione is safeguarded by additional reduction and transport systems. *New Phytologist* **224**, 1569–1584.

Marty L, Siala W, Schwarzländer M, Fricker MD, Wirtz M, Sweetlove LJ, Meyer Y, Meyer AJ, Reichheld JP, Hell R. 2009. The NADPH-dependent thioredoxin system constitutes a functional backup for cytosolic glutathione reductase in *Arabidopsis*. *Proceedings of the National Academy of Sciences of the United States of America* **106**, 9109–9114.

Mashiguchi K, Tanaka K, Sakai T, et al. 2011. The main auxin biosynthesis pathway in *Arabidopsis*. *Proceedings of the National Academy of Sciences* **108**, 18512–18517.

Meijering E, Jacob M, Sarria J-CF, Steiner P, Hirling H, Unser M. 2004. Design and Validation of a Tool for Neurite Tracing and Analysis in Fluorescence Microscopy Images. *Cytometry* **58**, 167–176.

Meyer Y, Belin C, Delorme-Hinoux V, Reichheld J-P, Riondet C. 2012. Thioredoxin and glutaredoxin systems in plants: molecular mechanisms, crosstalks, and functional significance. *Antioxidants & redox signaling* **17**, 1124–60.

Meyer AJ, Brach T, Marty L, Kreye S, Rouhier N, Jacquot J-P, Hell R. 2007. Redox-sensitive GFP in *Arabidopsis thaliana* is a quantitative biosensor for the redox potential of the cellular glutathione redox buffer. *The Plant journal : for cell and molecular biology* **52**, 973–86.

Mhamdi A, Hager J, Chaouch S, et al. 2010. *Arabidopsis* GLUTATHIONE REDUCTASE1 Plays a Crucial Role in Leaf Responses to Intracellular Hydrogen Peroxide and in Ensuring Appropriate Gene Expression through Both Salicylic Acid and Jasmonic Acid Signaling Pathways. *Plant Physiology* **153**, 1144–1160.

Michniewicz M, Ho C-H, Enders TA, et al. 2019. TRANSPORTER OF IBA1 Links Auxin and Cytokinin to Influence Root Architecture. *Developmental Cell*.

Moreno-Risueno MA, Van Norman JM, Moreno A, Zhang J, Ahnert SE, Benfey PN. 2010. Oscillating Gene Expression Determines Competence for Periodic *Arabidopsis* Root Branching. *Science* **329**, 1306–1311.

Nacry P, Canivenc G, Muller B, Azmi A, Onckelen H Van, Rossignol M, Doumas P. 2005. A Role for Auxin Redistribution in the Responses of the Root System Architecture to Phosphate Starvation in *Arabidopsis*. *Plant Physiology* **138**, 2061–2074.

Noctor G, Mhamdi A, Chaouch S, Han YI, Neukermans J, Marquez-garcia B, Queval G, Foyer CH. 2012. Glutathione in plants : an integrated overview. *Plant, Cell and Environment* **35**, 454–484.

- Noctor G, Reichheld J, Foyer CH.** 2018. ROS-related redox regulation and signaling in plants. *Seminars in Cell and Developmental Biology* **80**, 3–12.
- Orman-ligeza B, Parizot B, Rycke R De, Fernandez A, Himschoot E, Breusegem F Van, Bennett MJ, Pe C, Beeckman T, Draye X.** 2016. RBOH-mediated ROS production facilitates lateral root emergence in *Arabidopsis*. *Development* **143**, 3328–3339.
- Parisy V, Poinssot B, Owsianowski L, Buchala A, Glazebrook J, Mauch F.** 2007. Identification of PAD2 as a gamma-glutamylcysteine synthetase highlights the importance of glutathione in disease resistance of *Arabidopsis*. *The Plant journal : for cell and molecular biology* **49**, 159–72.
- Parry G.** 2018. Low Phosphate Puts Auxin in the Root Hairs. *Trends in Plant Science* **23**, 845–847.
- Péret B, Li G, Zhao J, et al.** 2012. Auxin regulates aquaporin function to facilitate lateral root emergence. *Nature Cell Biology* **14**, 991–998.
- Poitout A, Martinière A, Kucharczyk B, et al.** 2017. Local signalling pathways regulate the *Arabidopsis* root developmental response to *Mesorhizobium loti* inoculation. *Journal of Experimental Botany* **68**, 1199–1211.
- Pye VE, Christensen CE, Dyer JH, Arent S, Henriksen A.** 2010. Peroxisomal plant 3-ketoacyl-CoA thiolase structure and activity are regulated by a sensitive redox switch. *Journal of Biological Chemistry* **285**, 24078–24088.
- Queval G, Issakidis-Bourguet E, Hoerberichts FA, Vandorpe M, Gakière B, Vanacker H, Miginiac-Maslow M, Van Breusegem F, Noctor G.** 2007. Conditional oxidative stress responses in the *Arabidopsis* photorespiratory mutant *cat2* demonstrate that redox state is a key modulator of daylength-dependent gene expression, and define photoperiod as a crucial factor in the regulation of H₂O₂-induced cel. *Plant Journal* **52**, 640–657.
- Rahman I, Kode A, Biswas SK.** 2007. Assay for quantitative determination of glutathione and glutathione disulfide levels using enzymatic recycling method. *Nature Protocols* **1**, 3159–3165.
- Reichheld J-P, Khafif M, Riondet C, Droux M, Bonnard G, Meyer Y.** 2007. Inactivation of thioredoxin reductases reveals a complex interplay between thioredoxin and glutathione pathways in *Arabidopsis* development. *The Plant cell* **19**, 1851–65.
- Roman G, Lubarsky B, Kieber JJ, Rothenberg M, Ecker R.** 1995. Genetic analysis of ethylene signal transduction in *Arabidopsis thaliana*: five novel mutant loci integrated into a stress response pathway. *Genetics* **139**, 1393–1409.
- Ruffel S, Gojon A.** 2017. Systemic nutrient signalling: On the road for nitrate. *Nature Plants* **3**, 17040.
- Ruzicka K, Strader LC, Bailly A, et al.** 2010. *Arabidopsis* PIS1 encodes the ABCG37 transporter of auxinic compounds including the auxin precursor indole-3-butyric acid. *Proceedings of the National Academy of Sciences of the United States of America* **107**, 10749–53.
- De Rybel B, Audenaert D, Xuan W, et al.** 2012. a role for the root cap in root branching revealed by the non-auxin probe naxillin. *Nature Chemical Biology* **8**, 798–805.
- Saini S, Sharma I, Kaur N, Pati PK.** 2013. Auxin: a master regulator in plant root development. *Plant cell reports* **32**, 741–57.
- Shanmugam V, Tsednee M, Yeh K-C.** 2012. ZINC TOLERANCE INDUCED BY IRON 1 reveals the importance of glutathione in the cross-homeostasis between zinc and iron in *Arabidopsis thaliana*. *The Plant journal* **69**, 1006–17.
- Sherp AM, Westfall CS, Alvarez S, Jez JM.** 2018. *Arabidopsis thaliana* GH3.15 acyl acid amido synthetase

has a highly specific substrate preference for the auxin precursor indole-3-butyric acid. *Journal of Biological Chemistry* **293**, 4277–4288.

Simon S, Petrášek J. 2011. Why plants need more than one type of auxin. *Plant science : an international journal of experimental plant biology* **180**, 454–60.

Singh R, Singh S, Parihar P, Mishra RK, Tripathi DK, Singh VP, Chauhan DK, Prasad SM. 2016. Reactive Oxygen Species (ROS): Beneficial Companions of Plants ' Developmental Processes. *Frontiers in Plant Science* **7**, 1299.

Stanley CE, Shrivastava J, Brugman R, Heinzemann E, van Swaay D, Grossmann G. 2018. Dual-flow-RootChip reveals local adaptations of roots towards environmental asymmetry at the physiological and genetic levels. *New Phytologist* **217**, 1357–1369.

Stein M, Dittgen J, Sánchez-Rodríguez C, Hou B, Molina A, Schulze-iefert P, Lipka V, Somerville S. 2006. PLANT FUNGAL INFECTION PROCESS Arabidopsis PEN3 / PDR8 , an ATP Binding Cassette Transporter , Contributes to Nonhost Resistance to Inappropriate Pathogens That Enter by Direct Penetration. *The Plant Cell* **18**, 731–746.

Strader LC, Bartel B. 2009. The Arabidopsis PLEIOTROPIC DRUG RESISTANCE8/ABCG36 ATP binding cassette transporter modulates sensitivity to the auxin precursor indole-3-butyric acid. *The Plant cell* **21**, 1992–2007.

Strader LC, Bartel B. 2011. Transport and metabolism of the endogenous auxin precursor indole-3-butyric Acid. *Molecular plant* **4**, 477–86.

Strader LC, Culler AH, Cohen JD, Bartel B. 2010. Conversion of endogenous indole-3-butyric acid to indole-3-acetic acid drives cell expansion in Arabidopsis seedlings. *Plant physiology* **153**, 1577–86.

Strader LC, Wheeler DL, Christensen SE, Berens JC, Cohen JD, Rampey RA, Bartel B. 2011. Multiple Facets of Arabidopsis Seedling Development Require Indole-3-Butyric Acid-Derived Auxin . *The Plant Cell* **23**, 984–999.

Tognetti VB. 2017. Redox regulation at the site of primary growth : auxin , cytokinin and ROS crosstalk. , 2586–2605.

Tognetti VB, Van Aken O, Morreel K, et al. 2010. Perturbation of Indole-3-Butyric Acid Homeostasis by the UDP-Glucosyltransferase UGT74E2 Modulates Arabidopsis Architecture and Water Stress Tolerance. *The Plant Cell* **22**, 2660–2679.

Tsakagoshi H. 2016. Control of root growth and development by reactive oxygen species. *Current Opinion in Plant Biology* **29**, 57–63.

Tyburski J, Dunajska K, Tretyn A. 2009. Reactive oxygen species localization in roots of Arabidopsis thaliana seedlings grown under phosphate deficiency. *Plant Growth Regulation* **59**, 27–36.

Ulmasov T, Murfett J, Hagen G, Guilfoyle TJ. 1997. Aux/IAA Proteins Repress Expression of Reporter Genes Containing Natural and Highly Active Synthetic Auxin Response Elements. *The Plant Cell* **9**, 1963–1971.

Vacheron J, Desbrosses G, Bouffaud ML, Touraine B, Moëgne-Loccoz Y, Muller D, Legendre L, Wisniewski-Dyé F, Prigent-Combaret C. 2013. Plant growth-promoting rhizobacteria and root system functioning. *Frontiers in Plant Science* **4**, 1–19.

Vernoux T, Wilson RC, Seeley KA, et al. 2000. The ROOT MERISTEMLESS1 / CADMIUM SENSITIVE2 Gene Defines a Glutathione-Dependent Pathway Involved in Initiation and Maintenance of Cell Division during Postembryonic Root Development. *The Plant Cell* **12**, 97–109.

Wang T, Li C, Wu Z, Jia Y, Wang H, Sun S, Mao C, Wang X. 2017. Abscisic Acid Regulates Auxin Homeostasis

in Rice Root Tips to Promote Root Hair Elongation. *Frontiers in Plant Science* **8**, 1–18.

Woodward AW, Bartel B. 2004. The Arabidopsis Peroxisomal Targeting Signal Type 2 Receptor PEX7 Is Necessary for Peroxisome Function and Dependent on PEX5. *Molecular Biology of the Cell* **16**, 573–583.

Xuan W, Audenaert D, Parizot B, et al. 2015. Root cap-derived auxin pre-patterns the longitudinal axis of the arabidopsis root. *Current Biology* **25**, 1381–1388.

Xuan W, Band LR, Kumpf RP, et al. 2016. Cyclic programmed cell death stimulates hormone signaling and root development in Arabidopsis. *Science* **351**, 384–387.

Zhang GZ, Jin SH, Jiang XY, Dong RR, Li P, Li YJ, Hou BK. 2016. Ectopic expression of UGT75D1, a glycosyltransferase preferring indole-3-butyric acid, modulates cotyledon development and stress tolerance in seed germination of Arabidopsis thaliana. *Plant Molecular Biology* **90**, 77–93.

Zolman BK, Martinez N, Millius A, Adham AR, Bartel B. 2008. Identification and characterization of Arabidopsis indole-3-butyric acid response mutants defective in novel peroxisomal enzymes. *Genetics* **180**, 237–251.

Zolman BK, Nyberg M, Bartel B. 2007. IBR3, a novel peroxisomal acyl-CoA dehydrogenase-like protein required for indole-3-butyric acid response. *Plant molecular biology* **64**, 59–72.

Zwiewka M, Bielach A, Tamizhselvan P, Madhavan S, Dobrev P, Vankova R, Ryad EE, Tan S. 2019. Root Adaptation to H₂O₂ -Induced Oxidative Stress by ARF-GEF BEN1- and Cytoskeleton-Mediated PIN2 Trafficking. *Plant and Cell Physiology* **60**, 255–273.

Accepted Manuscript

FIGURE LEGENDS

Figure 1. Glutathione specifically regulates root responses to IBA.

- A. Total glutathione content in 8-day-old wild-type (Col-0), *cad2* or *pad2* seedlings grown on standard ½ MS medium. Wild-type plants grown in the presence of 0.5 mM BSO were also assayed (BSO). Data represent the means of 3 biological repetitions.
- B. Emerged lateral root density of 10-day-old wild-type (Col-0), *cad2* or *pad2* plants grown on standard ½ MS medium and wild-type plants grown in the presence of 0.5 mM BSO (n>15).
- C. Emerged LR and LR primordia density of 10-day-old wild-type plants grown on standard ½ MS medium (control), or in the presence of different combinations of BSO 0.5 mM, IBA 10 µM and/or IAA 50 nM, as mentioned (n>15).
- D. Developmental stages of LR primordia of 6-day-old wild-type (Col-0), *cad2* or *pad2* seedlings 48 hours after gravistimulation on standard ½ MS medium supplemented (bottom panel) or not (top panel) with 10 µM IBA; wild-type plants grown in the presence of 0.5 mM BSO were also assayed (BSO). Data indicate the percentage of LRP in each developmental stage (n> 16) and are representative of 3 independent experiments.
- E. Pictures of representative 8-day-old wild-type plants grown on standard ½ MS medium, or in the presence of different combinations of BSO 0.5 mM, IBA 10 µM and/or IAA 50 nM, as mentioned.
- F. Quantification of root hair length of 8-day-old wild-type (Col-0), *cad2* or *pad2* mutant plants grown on standard ½ MS medium (Control), or in the presence of 50 nM IAA (IAA) or 10 µM IBA (IBA). Wild-type plants in the presence of 0.5 mM BSO (BSO) were also assayed (n>100).

Histograms represent the mean and error bars represent the standard deviation. Asterisks indicate a significant difference, based on a two-tailed Student t-test (** P≤0.001).

Figure2. Glutathione is critical for the IBA-derived IAA signalling in the basal meristem

- A. Representative Pictures of 8-day-old GUS-stained *DR5:GUS* plants grown on standard ½ MS medium (Control) or in the presence of 0.5 mM BSO (BSO), after a 24-hour long treatment with 10 µM IBA or 50 nM IAA as precised (n≥7).

- B. Quantification of GFP and Tomato fluorescent signals from 8-day-old expressing the *DR5:n3EGFP/DR5v2:ntdTomato* double reporter, and grown in the same conditions as A ($n \geq 7$).

Figure 3. IBA hyposensitivity phenotype is specific to GSH-depleted plants.

- A. Glutathione content in 8-day-old wild-type (Col-0), *cad2*, *gr1*, *ntra ntrb* or *cat2* seedlings grown on standard $\frac{1}{2}$ MS medium. Data represent the means of 3 biological repetitions. Reduced glutathione is represented in white (GSH) and oxidised glutathione in black (GSSG).
- B. Representative pictures ($n > 10$) of roGFP2 reporter line grown on standard $\frac{1}{2}$ MS medium (MS), submitted to a 30 min treatment with 1 mM H_2O_2 then to an additional 30 min treatment with 10 mM DTT (top panel). The bottom panel represents roGFP2 reporter plants grown on standard $\frac{1}{2}$ MS medium supplemented (IBA) or not (MS) with 10 μM IBA. Pictures are made from the ratio between the oxidised roGFP2 signal (excitation at 405 nm) and the reduced roGFP2 signal (excitation at 488 nm). Ratio values are represented in the color scale.
- C. Emerged lateral root density of 10-day-old wild-type (Col-0), *cad2*, *cat2*, *gr1* or *ntra ntrb* plants grown on standard $\frac{1}{2}$ MS medium or the presence of 10 μM IBA ($n > 16$).

Histograms represent the mean and error bars represent the standard deviation. Asterisks indicate a significant difference, based on a two-tailed Student t-test (* $P < 0.01$; ** $P < 0.001$).

Figure 4. IAA transport is not the target of glutathione.

- A. Emerged lateral root density of 10-day-old wild-type (Col-0), *aux1* or *pin2* plants grown on standard $\frac{1}{2}$ MS medium, or in the presence of different combinations of BSO 0.5 mM and IBA 10 μM ($n > 10$).
- B. Emerged lateral root density of 10-day-old wild-type (Col-0) grown on standard $\frac{1}{2}$ MS medium, supplemented or not with the transport inhibitors NPA 1 μM or NOA 1 μM ($n \geq 15$).

Histograms represent the mean and error bars represent the standard deviation. Asterisks indicate a significant difference, based on a two-tailed Student t-test (** $P < 0.001$).

Figure 5. IBA homeostasis does not display sensitivity to glutathione.

- A. Uptake of [³H]IBA by wild type (Col), *cad2-1*, or *pdr9-1* excised root tips of 8-day-old plants. Data represent eight replicates with five root tips per genotype and per replicate.
- B. Emerged lateral root density of 10-day-old wild-type (Col-0), *pdr8*, *pdr9* or *pdr8 pdr9* plants grown on standard ½ MS medium, or in the presence of different combinations of BSO 0.5 mM and IBA 10 µM (n≥15).
- C. Emerged lateral root density of 10-day-old wild-type (Col-0), *ugt74e2*, *ugt74d1* or *ugt74e2 ugt74d1* plants grown on standard ½ MS medium, or in the presence of different combinations of BSO 0.5 mM and IBA 10 µM (n≥15).

Histograms represent the mean and error bars represent the standard deviation. Asterisks indicate a significant difference, based on a two-tailed Student t-test (*P<0,05; **P<0,001).

Figure 6. IBA conversion to IAA does not display sensitivity to glutathione.

- A. Emerged lateral root density of 10-day-old wild-type (Col-0), *ibr1*, *ibr3*, *ibr10*, *ibr1 ibr3 ibr10* or *ech2* plants grown on standard ½ MS medium, or in the presence of different combinations of BSO 0.5 mM and IBA 10 µM (n≥15).
- B. Expression levels (qRT-PCR) of *IBR1*, *IBR3*, *IBR10*, *ECH2*, *AIM1* and *PED1* genes in *cad2* relative to wild-type 8-day-old plants grown on standard ½ MS medium. Data represent three independent replicates with 20 plants per replicate.

Histograms represent the mean and error bars represent the standard deviation. Asterisks indicate a significant difference, based on a two-tailed Student t-test (*P<0,01; **P<0,001).

Figure7. Glutathione and IBA are specifically required for RH growth response to low phosphate.

- A. RH length in 8-day-old wild-type (Col-0), *cad2* or *ibr1 ibr3 ibr10* plants grown on standard ½ MS medium in the absence or the presence of the PGPR *Mesorhizobium loti* (see material and methods).
- B. RH length in 8-day-old wild-type (Col-0), *cad2* or *ibr1 ibr3 ibr10* plants grown on 3/10 MS medium supplemented with 500 µM sodium phosphate (control) or 500 µM sodium chloride (minusP).
- C. Expression levels (qRT-PCR) of *PHT1;4*, *RNS1* and *SPX1* low-phosphate responsive genes, relatively to *ACT2* control gene, in wild-type (Col-0), *cad2* or *ibr1 ibr3 ibr10* 8-day-old plants grown on 1/3 MS medium supplemented with 500 µM

NaH₂PO₄ (control) or 500 μM NaCl (minusP). Data represent three independent replicates with 20 plants per replicate and are normalized relatively to the wild-type value in control condition.

Histograms represent the mean and error bars represent the standard deviation. Asterisks indicate a significant difference, based on a two-tailed Student t-test (*P<0,01; **P<0,001).

Accepted Manuscript

Figure 1

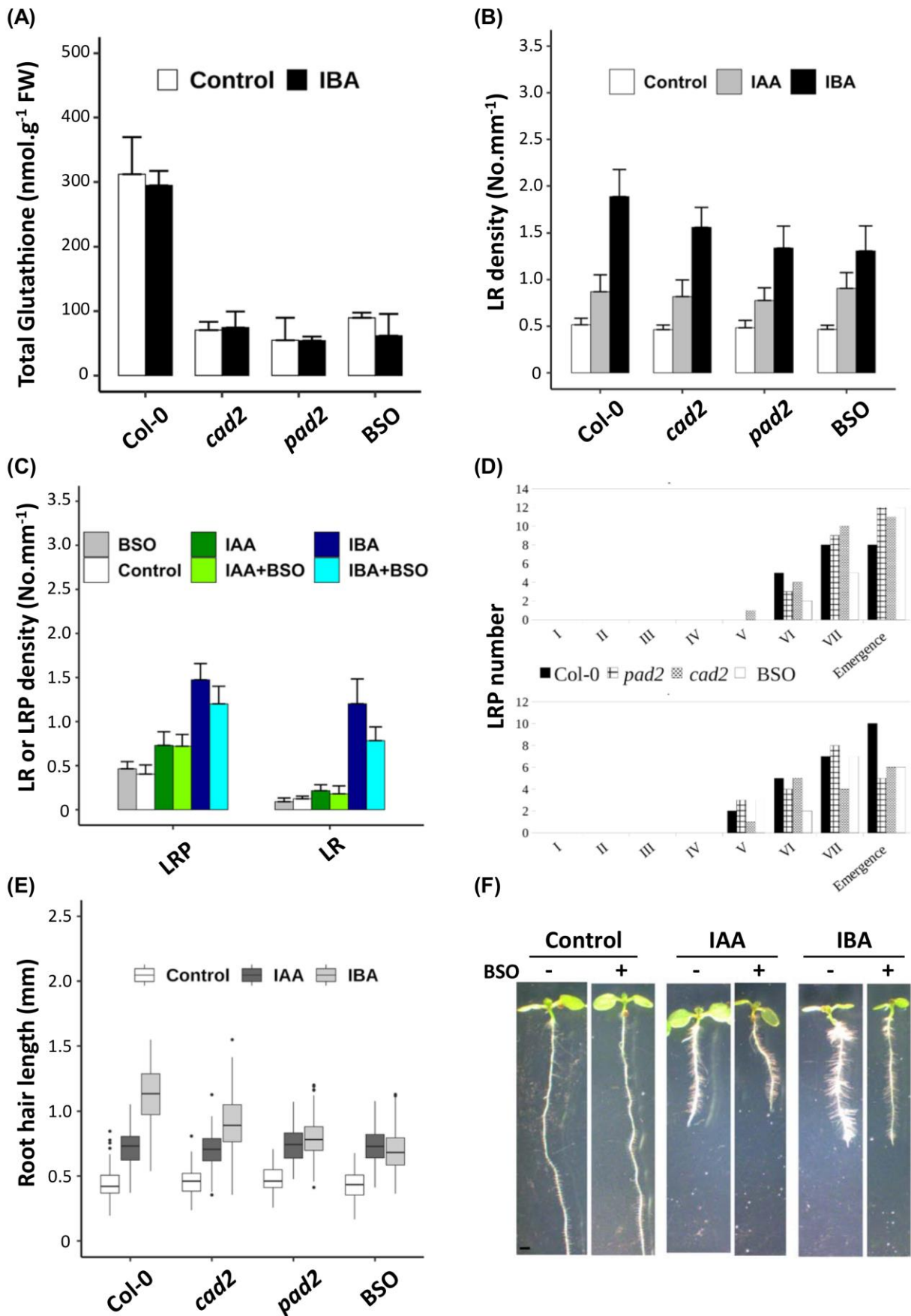


Figure 2

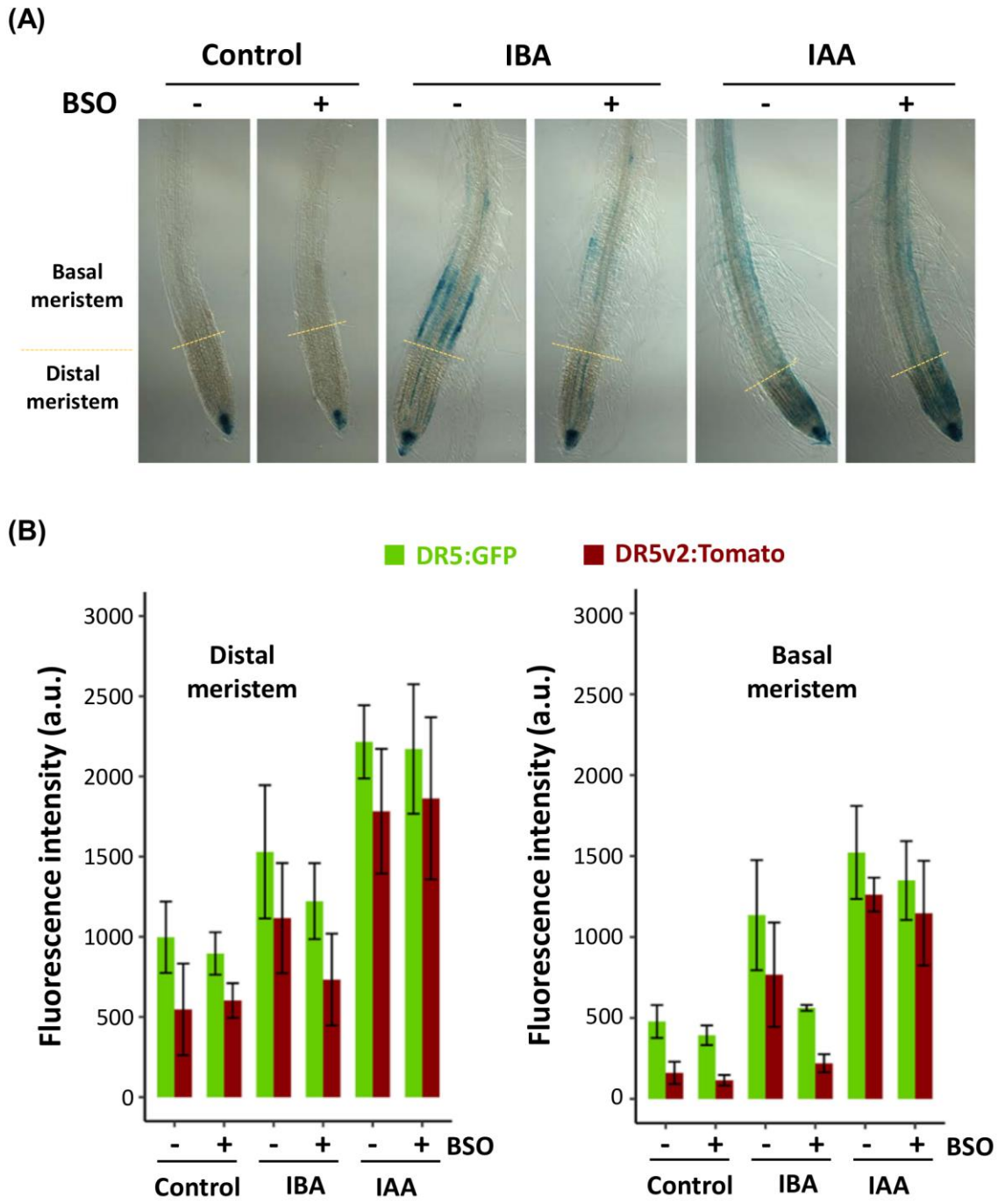
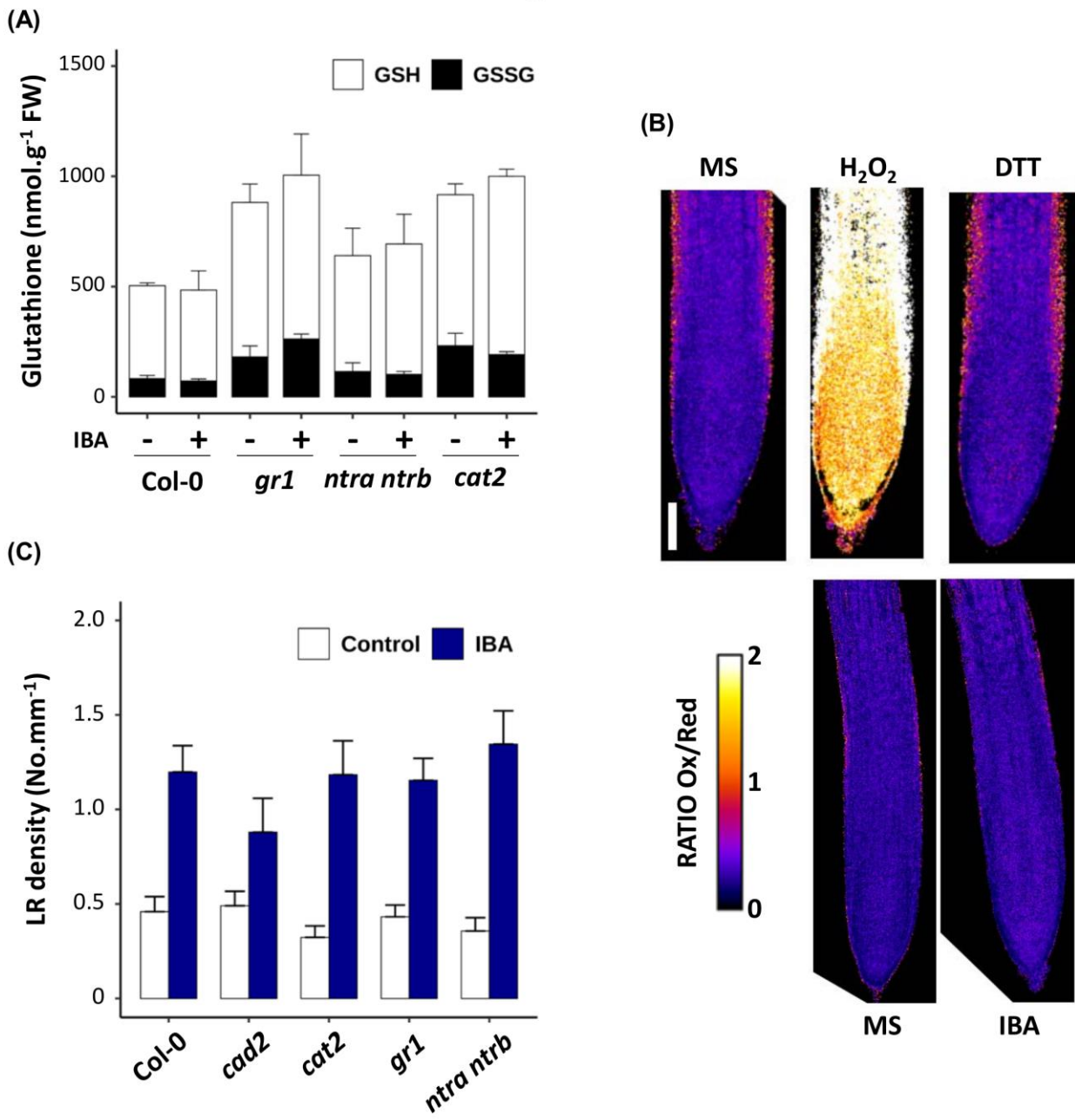
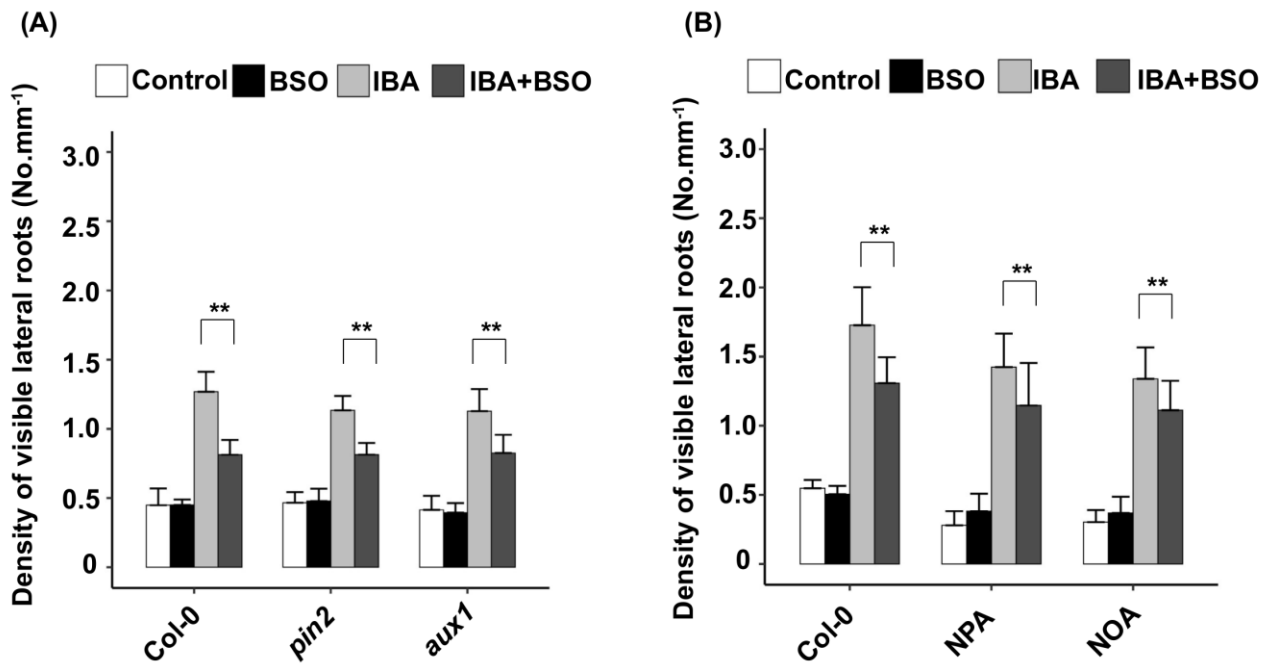


Figure 3



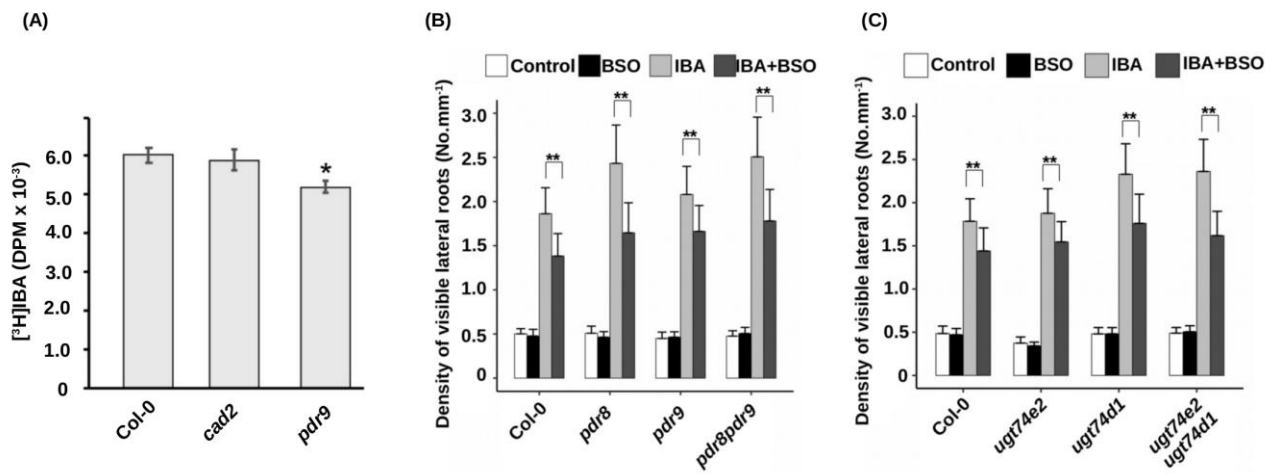
ACU

Figure 4



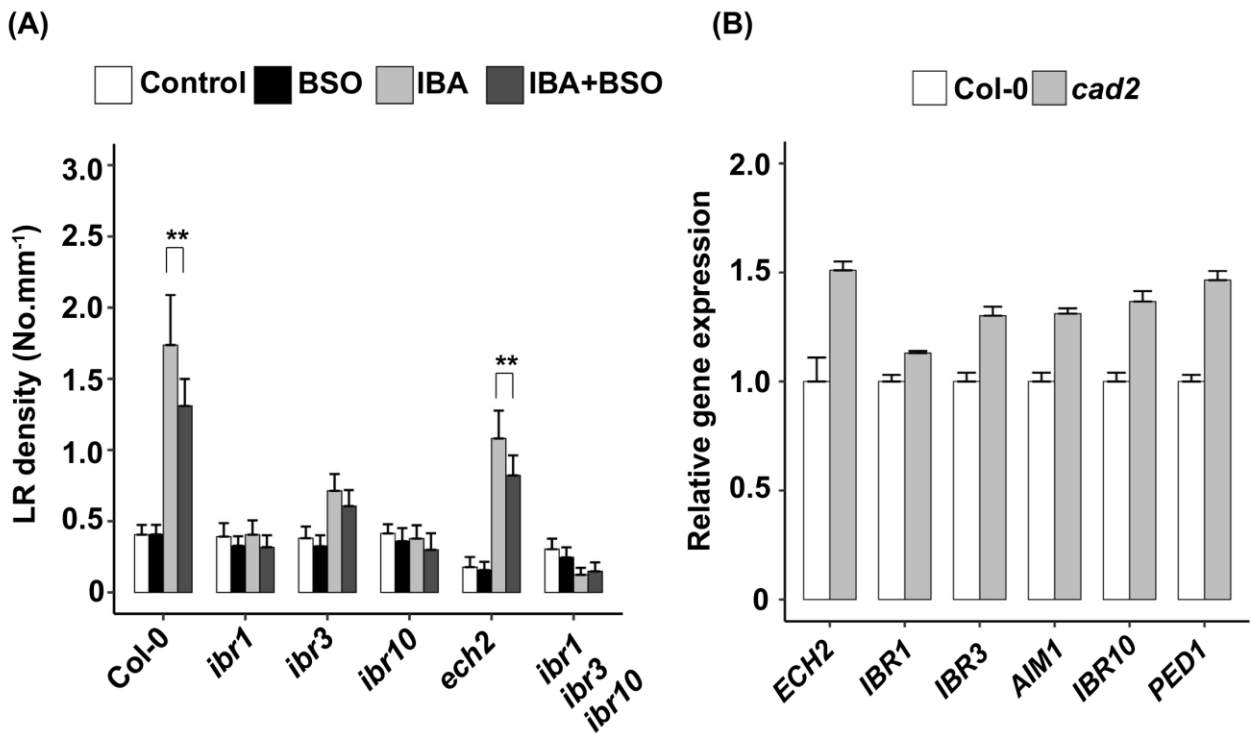
Accepted Manuscript

Figure 5



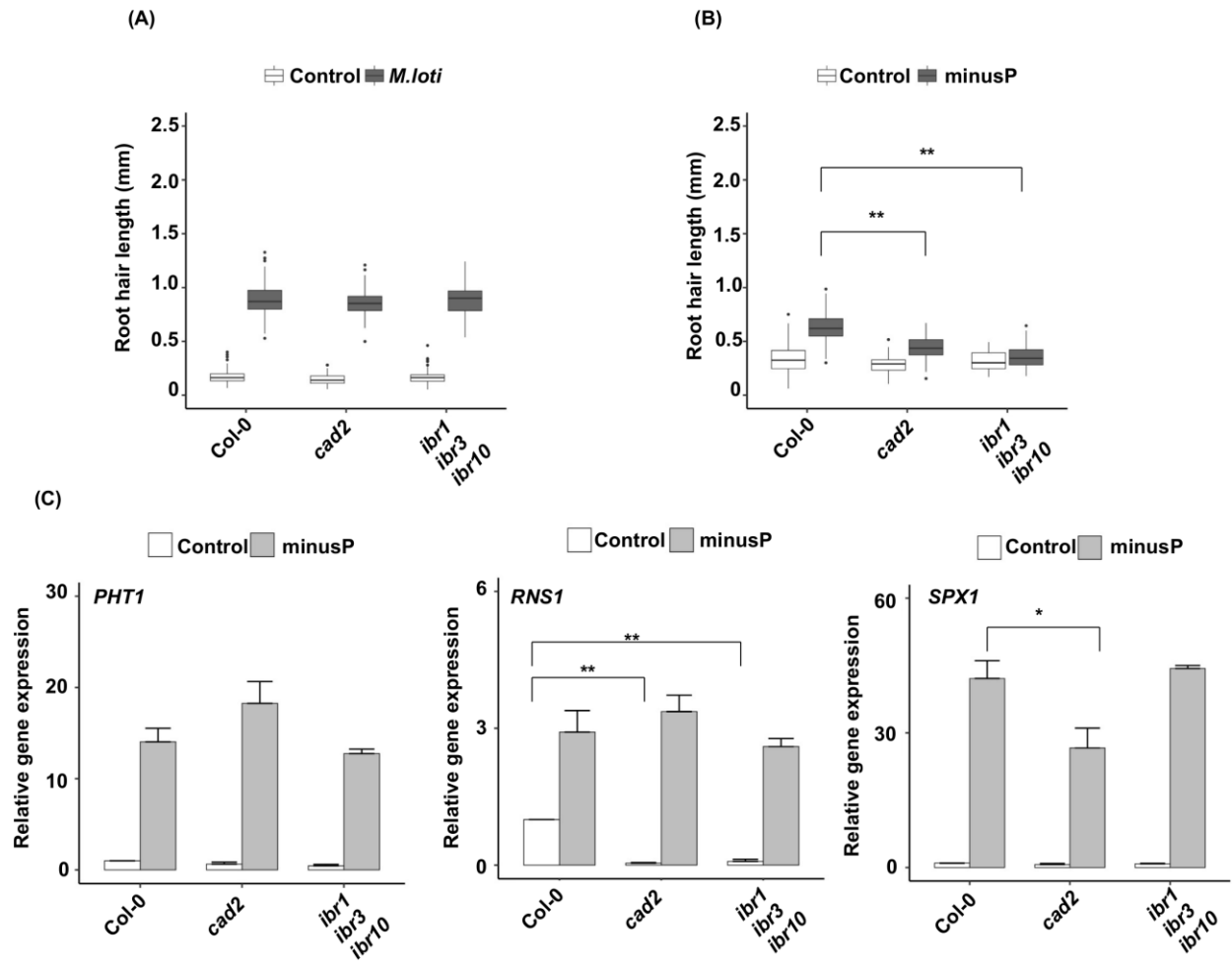
Accepted Manuscript

Figure 6



Accepted Manuscript

Figure 7



Accepted